

# Absolute Ranging for Maritime Applications using TerraSAR-X and TanDEM-X Data

Sergi Duque<sup>1</sup>, Ulrich Balss<sup>1</sup>, Xiao Ying Cong<sup>2</sup>, Nestor Yague-Martinez<sup>2</sup> and Thomas Fritz<sup>1</sup>

<sup>1</sup> German Aerospace Center (DLR). Remote Sensing Technology Institute.

<sup>2</sup> Technische Universitat Munchen (TUM), Chair of Remote Sensing Technology.

Email: Sergi.DuqueBiarge@dlr.de

## Abstract

The SAR geolocation accuracy using TerraSAR and TanDEM-X data has been demonstrated to be into centimeter level with no need of any reference frame. This paper is intended to show potential applications over maritime scenarios based on precise absolute measurements. Two specific applications are discussed and analyzed. The first one is to measure ships 2D velocity using TanDEM-X products. The second application is monitoring possible offshore platforms displacements using TerraSAR and TanDEM-X data.

## 1 Introduction

The unprecedented geometric accuracy of the German SAR satellites TerraSAR-X and TanDEM-X raises a new perspective in SAR geolocation. Their orbits are determined with a 3-D accuracy of 4.2 cm in the precise science orbit product [1]. This fact has encouraged the pursuit of the finest possible SAR geolocation using TerraSAR-X and TanDEM-X data. Recent works have demonstrated that the pixel geolocation accuracy can be in the cm level [2, 3] or even in the mm level [4]. As a natural step, the focus of the present paper is to exploit this unprecedented SAR geolocation accuracy for change detection applications where there is no frame reference. Thus, maritime scenarios have a huge potential for absolute ranging applications. This paper presents two specific maritime applications. The first application takes advantage of the along track (AT) baseline of TanDEM-X bistatic data to derive 2D ship's velocity. The second one is related to precisely monitor the absolute displacement of offshore platforms using TerraSAR-X repeat-pass data.

## 2 Ship 2D absolute velocity estimation

The small temporal lag between TanDEM-X single-pass acquisition channels can be used to detect moving targets and measure their velocity. The AT baselines in the TanDEM-X close formation are in the range of set of tens to few hundreds meters. The ATI phase gets wrapped for velocities in the order of few meters per second. Therefore, the ATI approach is unfeasible to get absolute velocities. This paper analyses an alternative to ATI for ship velocity estimation using TanDEM-X products. The approach is based on cross-correlation between two channels from a single TanDEM-X acquisition. Thus, the derived velocity is a 2D vector with range and azimuth com-

ponents. The TanDEM-X image pair present an along and across-track baseline components. Due to the across-track baseline and the unknown interferometric fringes produced by unknown ship's height, the incoherent cross-correlation is choose instead of coherent. In general, the cross-correlation displacement accuracy depends on how big is the estimation window and the obtained coherence. In [5], the accuracy of incoherent cross-correlation for circular gaussian signals is derived in terms of resolution units as

$$\sigma_I = \sqrt{\frac{3}{2N_{eff}} \frac{\sqrt{2 + 5\gamma^2 - 7\gamma^4}}{\pi\gamma}}, \quad (1)$$

where  $\gamma$  is the cross-correlation coherence and  $N_{eff}$  is the number of independent looks. However, our specific scenario is far away from circular gaussian signals. In our case, the backscattered signal comes from man-made structures which produce a combination of defined features and point target responses. Thus, (1) is not any accuracy bound and it can just give an idea of the expected accuracy magnitude order. The accuracy depends strongly on the image features and its contrast with the clutter. The cross-correlation measure also contains the tropospheric and ionospheric differential delay, the impact of a priori wrong height estimation and the relative orbit accuracy. The differential tropospheric and ionospheric delays can be derived from [2] as function of the normal baseline as

$$\begin{aligned} \Delta\delta_{tropo} &= \delta_{tropo,sea} e^{-h/h_0} \frac{\tan(\theta)}{R \cdot \cos(\theta)} \cdot B_{n,eff} \\ \Delta\delta_{iono} &= \frac{40.28m^3s^{-2}}{f^2} \frac{VTEC \cdot \tan(\theta)}{R \cdot \cos(\theta)} \cdot B_{n,eff}, \end{aligned} \quad (2)$$

where  $\delta_{tropo,sea}$  is the tropospheric zenith delay at sea level,  $h$  is the height above sea level,  $h_0$  is the atmospheric thickness,  $f$  denotes the carrier frequency,  $VTEC$  is the Vertical Total Electron Content,  $R$  is the range to master satellite,  $\theta$  is the incidence angle and  $B_{n,eff}$  is

the normal effective baseline. The expected geometric shifts between the two images are calculated taking into account the orbits and a priori DEM. However, it may exist a mismatch between the used DEM and the real height of the targets of interest. This height error is due to a priori wrong estimation of the sea level height and unknown ships' heights. This effect introduces a bias in the range displacement measured by cross-correlation. It can be expressed as

$$\delta_{h_{err}} = \frac{B_{n,eff}}{R \cdot \sin(\theta)} \cdot h_{err}, \quad (3)$$

being  $h_{err}$  the height error. The described  $\delta_{h_{err}}$ ,  $\Delta\delta_{tropo}$  and  $\Delta\delta_{iono}$  derive in a bias in the range direction.

In order to show the potential of this application, a first result is illustrated on this paper. The test site is the Strait of Gibraltar and the used data is Alternating Bistatic (AB) TanDEM-X data in a Strip Map acquisition mode. The use of AB data provides a larger AT baseline and consequently a better sensitivity. **Table 1** lists the relevant acquisition and cross-correlation processing parameters.

$B_{n,eff}$	289.5 m	$R$	730.2 Km
$B_{AT}$	363.1 m	$\theta$	47.2°
$rg_{res}$	1.18 m	$\tau_{AT}$	51 ms
$az_{res}$	3.3 m	$\gamma_{th}$	0.9
$\tau_{AT}$	51 ms	XC Window	32x32 pix
		$N_{eff}$	579.2

**Table 1:** Relevant acquisition and processing parameters for ship velocity estimation.

The employed cross-correlation sliding window size is 32 by 32 pixels, which corresponds to a spatial extension in slant range - azimuth of 29.1 by 77.3 meters. According to the parameters in **Table 1** and assuming a reasonable values of height error and tropospheric delay at sea surface of 20 and 2.5 meters respectively, the expected displacement and velocity errors are depicted in **Table 2**.

	Displacement	Velocity
$\sigma_{I,rg}$	2.55 cm	1.8 Km/h
$\sigma_{I,az}$	7.17 cm	5.06 Km/h
$\Delta\delta_{tropo}$	1.58 mm	0.11 Km/h
$\Delta\delta_{iono}$	13.6 $\mu$ m	$10^{-3}$ Km/h
$\delta_{h_{err}}$	1.1 cm	0.21 Km/h

**Table 2:** Theoretical accuracy and bias in terms of displacement and velocity.

The cross-correlation accuracies,  $\sigma_{I,rg}$  and  $\sigma_{I,az}$ , have been calculated using (1). Therefore, as said before, these values just give a magnitude order and they can not be considered as accuracy boundaries.

In order to have an estimation of the relative orbit accuracy in the AT direction, the estimated azimuth offset between the signal measured cross-correlation and the a priori geometric shift for all the operational TanDEM-X bistatic pairs of the year 2013 has been statistically analyzed. This parameter contains mainly errors due to orbit

and timestamps inaccuracies. Its histogram is shown in **Figure 1**.

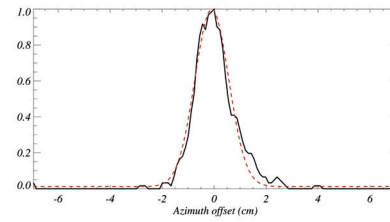


**Figure 1:** TanDEM-X estimated azimuth offset histogram.

The histogram is plotted in solid black line and its gaussian fit in dashed red. The gaussian fit has a mean of 0.1 cm and a standard deviation of 0.7 cm. The two channels used in this paper to measure ship displacement are both monostatic from an AB acquisition. Therefore, the expected displacement offset is twice the bistatic,  $\sigma_{az,orb} = 1.4$  cm, and its corresponding velocity is  $\sigma_{V_{az,orb}} = 1.0$  Km/h.

In our case, the imaged scene contains a land area which can be used to estimate the azimuth and range offsets between cross-correlation and a priori geometric shifts. These range and azimuth offsets are 1.2 mm and 2.4 cm respectively which taking into account the temporal lag yields a velocity bias of 0.08 Km/h in range and 1.71 Km/h in azimuth. The range offset main contribution is due to the differential tropospheric delay. The azimuth offset presents a higher value than azimuth offset standard deviation. This mismatch should be statistically analyzed for AB acquisition.

The derived range velocities are illustrated in **Figure 2** for the whole scene. It can be observed that the land remains at a 0 Km/h constant velocity after the offset correction while the detected ships show a non zero velocity.

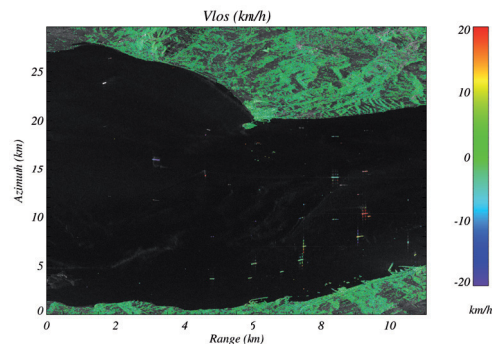


**Figure 2:** Derived line of sight velocities.

As an example, the derived velocity for the ship illustrated in **Figure 3** is analyzed. The white arrow is the heading angle extracted from ship shape, it can be also seen the wake of the ship which remains at the true ship position. Therefore, taking into account the azimuth ship displacement, it is possible to get a rough estimation of the ship range velocity, around 23.2 Km/h. The cross-

correlation displacements are converted to velocities, statistically analyzed and an outlier rejection is performed. The histogram is shown on **Figure 4**. The obtained range and azimuth velocities are  $-22.7 \text{ Km/h}$  in range, which matches the expected rough estimation using the wake position, and  $15.5 \text{ Km/h}$  in azimuth. Taking into account the the number of independent cross-correlations is 12.1, the range and azimuth velocity accuracies yield  $0.8 \text{ Km/h}$  and  $2.7 \text{ Km/h}$  respectively. Both heading angles are within the confidence interval.

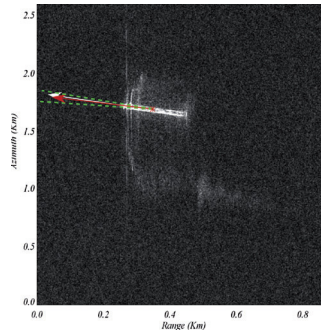


**Figure 3:** Ship with its heading angle derived from ship shape (white arrow) and the estimated heading angle in red arrow with its confident error in dashed green.

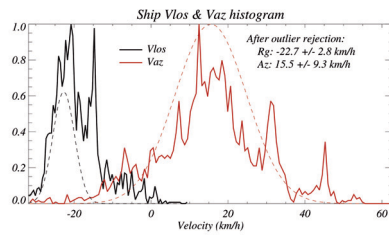


**Figure 4:** Histogram of range (black) and azimuth (red) velocities.

### 3 Platform monitoring over the sea

Offshore platforms are man made structures isolated on the sea. Therefore, there is a lack of reference for SAR techniques to monitor the stability of this structures. This paper analyzes the suitability of absolute ranging techniques to monitor this kind of structures. The data to be employed is repeat-pass from TerraSAR-X and TanDEM-X satellites. Since the platforms are at a specific position and their extension is relatively small compared to SAR image coverage, makes sense to use High Resolution (HS) or even Staring Spotlight (ST) images in order to obtain a better cross-correlation accuracy. The choose test-site corresponds to the offshore platform Helwin1. This platform attached to the seabed was installed by Siemens in the North Sea in August 2013. It will convert the alternating current power generated by wind turbines into low-loss direct current for transmission to land, it will be operative during 2014. As it can be seen on **Figure 5**, Helwin1 is far away from any land, the closest

land is more than 40 Km away.



**Figure 5:** Helwin1 offshore platform.

The used data are two pair of ST TerraSAR-X images acquired on November 4th and 15th 2013. The relevant acquisition and processing parameters are depicted in **Table 3**.

$Az_{res}$	23 cm	$Rg_{res}$	58.3 cm
$R$	642.4 Km	$B_n$	82.0 m
$\theta$	45.3°	$\gamma_{th}$	0.9
$N_{eff}$	2288.5	CC Window	64 x 64 pix 29.1 x 10.6 m

**Table 3:** Relevant acquisition and processing parameters for offshore platform monitoring.

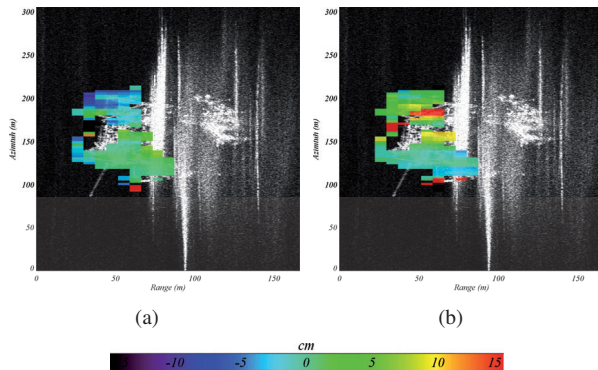
Taking into account these parameters and according to (1), the expected range and azimuth accuracies for circular gaussian signals are  $0.6 \text{ cm}$  and  $0.25 \text{ cm}$  respectively. Also, as in the previous application, the unknown platform height provokes a bias in the cross-correlation measure due to having a non zero normal baseline. A coarse height estimation can be derived from the SAR image taking into account the platform-water double bounce position respect the layover commence and the incidence angle. The coarse height estimation is  $45.4 \text{ m}$  which corresponds to cross-correlation range bias of  $0.8 \text{ cm}$ .

Other effects taken into account in this paper are tropospheric delay, Solid Earth Tides (SET) and Tidal Ocean Loading (TOL). When the images are not acquired in a single-pass, the tropospheric delay has the biggest impact in range direction. The tropospheric delay has been calculated using the 3-D numerical weather model data from the European Center for Medium-Range Weather Forecast (EMCMWF) [3]. The Solid Earth Tides are the most prominent geodynamic effect. They are caused due to the gravitational changes of the Sun and the Moon. Their impact is on the range and azimuth directions. The deformation of the Earth due to tidal changes of the mass ocean distribution has an important effect for offshore areas. The calculated differential tropospheric, SET and TOL impacts in range and azimuth direction are listed in **Table 3**.

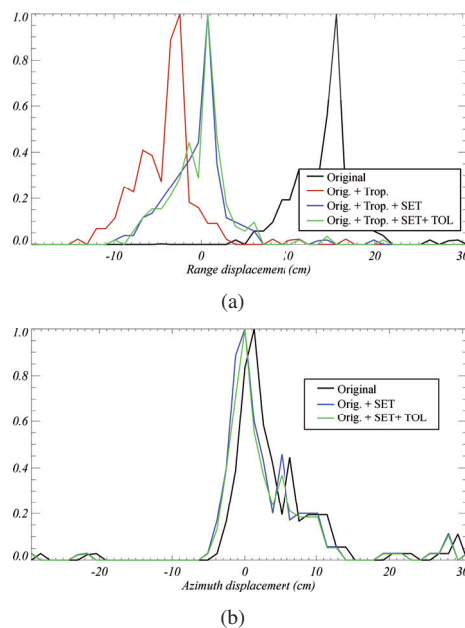
$\Delta\delta_{tropo}$	$Rg$	$Az$
$\Delta SET$	18.2 cm	0 cm
$\Delta TOL$	-3.6 cm	1.3 cm
	-2.7 mm	0.7 mm

**Table 4:** Calculated differential delays.

The measured cross-correlation shifts in range and azimuth directions after the described delay compensation are illustrated in **Figure 6** overlay over the master amplitude image.

**Figure 6:** Measured range and azimuth shifts.

The normalized histograms are shown in **Figure 7**.

**Figure 7:** Range and azimuth displacement histograms.

As it can be seen on **Figure 6**, the SAR image is significantly complex and presents multiple bounces and water interaction. Therefore, the number of reliable cross-correlations over the coherence threshold is quite reduced. In **Figure 7**, the measured cross correlation compensated with the a priori geometric shifts histogram is plotted in black. Then, histogram with tropospheric delay compensated is plotted in red. The SET delays are taken into account, blue histogram, and finally also TOL delays are also compensated, green histogram. After all the mentioned compensations, the mean and standard deviation for the cross-correlation in range direction are  $0.7\text{ cm}$  and  $1.1\text{ cm}$  respectively. The corresponding mean and

standard deviation for azimuth direction are  $0.3\text{ cm}$  and  $2.0\text{ cm}$  respectively. The obtained accuracy is able to detect platform displacements in the order of few centimeters. In order to be able to monitor the platform with accuracies below the centimeter level and to detect some possible displacement trends, a temporal series is needed.

## 4 Summary and conclusions

The SAR geolocation breakthrough presented in previous works using TerraSAR and TanDEM-X data arises the potential of change detection applications based on absolute ranging. This paper presents two SAR maritime applications with an absolute ranging approach where it is not possible to have a reference frame. In order to obtain precise change detection several effects have to be taken into account, such like signal travel path delays or geodynamic effects. The first application uses TanDEM-X products to measure absolute ships velocities. The accuracy of this measurements is below the kilometer per hour for relatively big ships. The second application consist in precise monitoring offshore platforms where there is no reference. This paper shows that is possible to monitor absolute displacements with accuracies around few centimeter. In order to be possible to detect some displacements patterns, it would be necessary the use of a temporal series.

## References

- [1] Y.T. Yoon, M. Eineder, N. Yague-Martinez, and O. Montenbruck. TerraSAR-X Precise Trajectory Estimation and Quality Assessment. *Geoscience and Remote Sensing, IEEE Transactions on*, 47(6):1859–1868, 2009.
- [2] M. Eineder, C. Minet, P. Steigenberger, Xiaoying Cong, and T. Fritz. Imaging Geodesy – Toward Centimeter-Level Ranging Accuracy With TerraSAR-X. *Geoscience and Remote Sensing, IEEE Transactions on*, 49(2):661–671, 2011.
- [3] Xiaoying Cong, U. Balss, M. Eineder, and T. Fritz. Imaging Geodesy – Centimeter-Level Ranging Accuracy With TerraSAR-X: An Update. *Geoscience and Remote Sensing Letters, IEEE*, 9(5):948–952, 2012.
- [4] U. Balss, C. Gisinger, Xiao Ying Cong, R. Brcic, P. Steigenberger, M. Eineder, R. Pail, M. Hugentobler, U. Eineder, and T. Fritz. High Resolution Geodetic Earth Observation with TerraSAR-X: Correction Schemes and Validation. In *Geoscience and Remote Sensing Symposium (IGARSS), 2013 IEEE International*, pages 4499–4502, 2013.
- [5] F. De Zan. Accuracy of incoherent Speckle Tracking for Circular Gaussian Signals. *Geoscience and Remote Sensing Letters, IEEE*, PP(99):1–1, 2013.